

WAVE TRANSMISSION IN MANGROVE FORESTS

by

Gerrit Jan Schiereck and Nico Booij
Delft University of Technology
P.O.Box 5048, 2600 GA Delft
The Netherlands

ABSTRACT

There is an increasing awareness of the role of mangrove forests in coastal ecosystems and coastal protection. At the transition between ocean and land, they have to absorb the energy that comes from the motion of the water. Little quantitative information is available, however, on wave transmission in these forests. In this paper the possibilities of the use of mathematical models to determine the influence of mangroves on waves are being explored. Both short and long waves have been examined. The results have also been used to try to say something on phenomena encountered in nature.

1. INTRODUCTION

Mangrove forests are the natural vegetation of many tropical coasts and tidal inlets and form a highly productive ecosystem, a maternity and nursery for many marine species. Living in very dynamic circumstances, mangrove trees are real miracles in surviving. They can cope with salt water where most other plants cannot. Seedlings have little opportunity to settle, so mangroves are viviparous, giving birth to an almost complete tree in a capsule (the propagule) that can travel with the tide and can turn into an upright standing young tree within a few days.

There is an increasing awareness of the importance and vulnerability of mangrove forests. These forests also play a role as a natural coastal protection and at places where they are removed for whatever reason, erosion and/or artificial protection is the price to be paid. The prospect of planting vegetable breakwaters, however, is not very promising. Mangroves can only exist on coasts with a moderate wave climate (Noakes, 1955). This is mainly caused by the fact that the seedlings cannot settle in highly dynamic conditions (Sato, 1985). Once the trees are grown up, however, they can even stand an occasional cyclone (Stoddart, 1965; Hopley, 1974).

There is a wealth of literature on mangroves, but little from a physical or coastal engineering point of view. This paper deals with wave damping in mangroves which forms a boundary condition for sedimentation and erosion and for biological activities. The approach is from an engineering point of view, using numerical wave models, trying to grab some natural phenomena in physical and mathematical descriptions. Both short and long waves are being studied in this paper. Examples of short waves on coasts with mangroves are mainly wind waves, including swell. Tsunamis, tides and storm surges are examples of long waves. Delft University of Technology (DUT) has several models available for the study of waves. The main purpose of this paper is to explore the possibilities of the use of these mathematical models for the study of wave transmission in vegetation, in particular mangrove trees. In the second place, we look for some insight in the influence of mangrove forests on wave transmission.

2. SOME CHARACTERISTICS OF MANGROVES

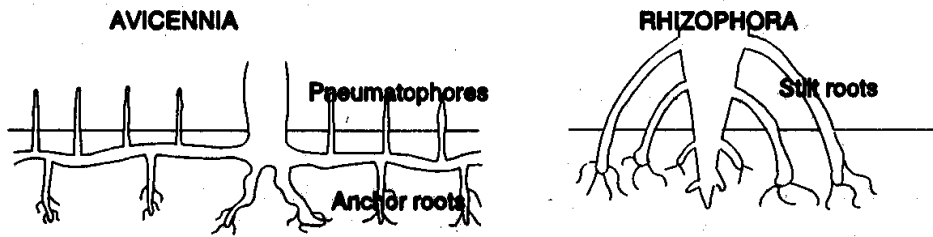


Figure 1 Root systems of Avicennia and Rhizophora mangroves

One of the most striking visible features of mangroves is the root system. Because of the anaerobic conditions in the mud soil on which mangroves usually live, they improve their gas exchange with the atmosphere by means of aerial roots. Of the many mangrove species in the world, we will deal in this paper with the two most important, viz. Avicennia and Rhizophora. Some authors report on Rhizophora mangrove forests with a seaward Avicennia fringe, others the other way around. These species have completely different aerial roots. Rhizophora works with "prop"-roots or "stilt"-roots, while Avicennia works with "snorkel"-type pneumatophores, emerging vertically from the bottom, see Figure 1. These roots play an important role in wave damping, probably even more than the trunks of the trees.

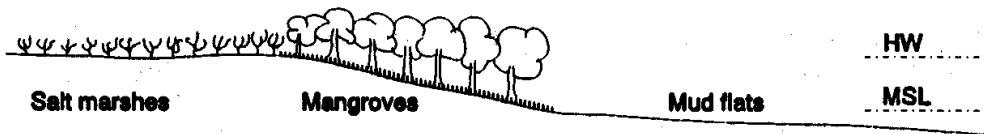


Figure 2 Possible cross-section of coast with mangroves

Because of this breathing system, mangrove trees need fresh air regularly and for this reason they can live only in the upper tidal zone, approximately above Mean Sea Level up to High Water (Spring). They can stand storm surges, but after extremely long periods of flooding, drowning of mangroves has been reported (Steinke and Ward, 1989) or even suffocating when large quantities of sediment have covered the root systems during a storm. Below MSL, the seedlings cannot settle and at higher levels, the mangroves cannot compete with other plant species. The coastline in front of mangroves often consist of mud flats, possibly covered with some pioneer seagrass vegetation (*Zostera*). Behind the mangroves, between HWS and the level of occasional flooding by the ocean, salt marshes can be found with halophytic (salt-loving) herbs and grasses, before the "normal" vegetation starts, see Figure 2. The width of these tidal forests is mainly determined by the tidal range (which can vary from a few decimeters to more than 5 meters along tropical coasts). The vegetation itself probably determines the slope of the bottom to a high degree, which will be discussed in this paper.

3. WIND WAVE TRANSMISSION AND THE HISWA PROGRAM

For the computation of wave transmission, the DUT-model HISWA (HIndcast Shallow water WAVes) is used (Holthuijsen et al., 1989). HISWA is based, in the cases described here, on a spectral energy balance:

$$\frac{\partial}{\partial x}(c_x E) + \frac{\partial}{\partial y}(c_y E) + \frac{\partial}{\partial \theta}(c_\theta E) = S \quad (1)$$

E is the variance density; variance is the wave energy divided by the density of the water and the acceleration of gravity. The first two terms describe the wave energy propagation in two horizontal directions, x and y , where c_x and c_y represent the propagation speed in x, y -space. The third term represents refraction, where c_θ is the propagation speed in wave direction, θ . The various source and sink terms are, in our case, limited to dissipation by wave breaking, bottom friction and resistance of mangrove trees. The surf dissipation is according to Battjes and Jansen, 1979 and the bottom dissipation to Putnam and Johnson, 1949. In this study only the behaviour of incoming waves, perpendicular to the coast, is studied. Refraction, wind and current are left out of consideration.

The wave energy dissipation by mangrove trunks and roots can be derived from the instantaneous rate of work done by the drag forces on a cylinder of incremental height dz (the work by the inertia force is assumed to be zero when averaged over a wave cycle):

$$dW = dF_D u = \frac{1}{2} \rho C_D D u^3 dz \quad (2)$$

The velocity u comes from linear wave theory. Integration over depth and wave period gives for the energy dissipation per m^2 bottom, given n cylinders per m^2 , see also Ippen, 1962:

$$S_C = \frac{2}{3\pi} n C_D D \frac{a^3 \omega^3}{gk} \left[\frac{1}{3} + \frac{1}{\sinh^2 kd} \right] \quad (3)$$

This sink term is implemented in the HISWA model with a modification to take into account irregular waves (the same way it was done for bottom friction, see Holthuijsen, 1989).

Bottom friction is described with:

$$\tau = \frac{1}{2} \rho C_F u_{bottom}^2 \quad (4)$$

For a bare bottom C_F is given by Jonsson, 1966 as a function of bottom roughness and orbital motion at the bottom, coupled to boundary layer growth under a wave. Note: The bottom friction coefficient in HISWA is defined as half the value of C_F in equation (4) and will be indicated as C_f in this paper. Mangrove roots will penetrate the boundary layer and their influence can be described with the above-mentioned cylinder approach. In that case C_f is determined by the total resistance force of the cylinders and becomes simply :

$$C_f = \frac{n C_D D L}{2} \quad (5)$$

To check the outcome of these formulae in the HISWA program, computational results were compared with some tests in a laboratory flume, from Groen, 1993. 30 cm high rods with a diameter of 0.9 cm were placed over a length of about 4 m, with a density of 200 and 400 rods/m². Tests were done with regular waves ($T = 0.8$ s to 1.5 s) in waterdepths of 0.25 m and 0.5 m. In the first case equation (3) could be tested, in the second case equation (5).

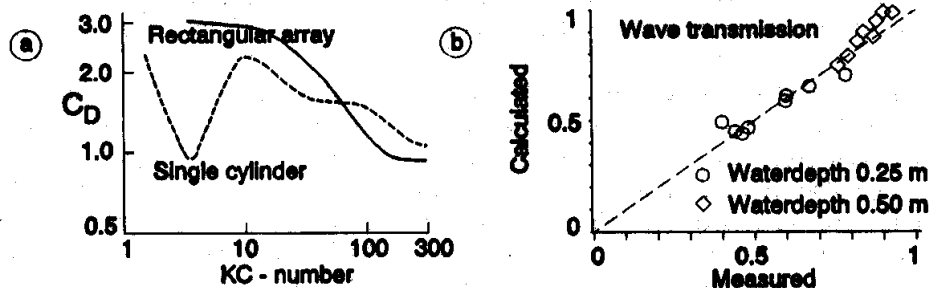


Figure 3 a: Influence KC-number on C_D -values; b: comparison of wave transmission coefficients computed with HISWA and measured in flume tests

In both cases, a C_D -value for the rods is needed which depends, among other things, on the Keulegan Carpenter number ($= \hat{u}T/D$) and the spacing of the cylinders. Heidemann and Sarpkaya, 1985 found for a rectangular array of cylinders the relation presented in Figure 3a, which was used in the hindcast of the experimental results. Figure 3b shows the comparison of the computed and measured values of the wave transmission, which is quite reasonable.

4. COMPUTATIONS OF WIND WAVE TRANSMISSION

The resistance against flow and waves of mangrove trees, has to be schematized in HISWA with the friction factor C_f , via equation (5), for pneumatophores, and with the pile resistance equation (3) for trunks. Since the density of trees and roots varies considerably, at first a possible range for these factors is estimated. Very little quantitative information is available, so only rough estimates can be made.

Snedaker and Snedaker, 1985 give some information on the number of trunks per surface area for mangrove forests (derived from various locations in the new world). There is a decrease in density as the trees become older and thicker, while the total volume of wood per area remains about constant. The relation between trunk diameter (m) and density ($1/m^2$) according to Snedaker and Snedaker, 1985 is approximated here with:

$$n = 0.007 D^{-1.5} \quad (6)$$

Since the effect of n , C_D and D in equation (3) comes from the product of the three parameters, it has little use to study the effect of each separately. Equation (6) is applied with trunk diameters ranging from 0.05 to 0.25 m yielding $n \cdot D \approx 0.03$ and 0.015 respectively. C_D for the small diameter will not differ much from unity, while for the large trunks it can, according to Figure 3a, vary between 1 and 3, depending on the wave period. So, as possible values for the product $n \cdot C_D \cdot D$, a range of 0.01 - 0.05 is assumed.

Spenceley, 1977 and Bird, 1980 give some information on density of pneumatophores of Avicennia. Near the trunk, densities of 400 - 500/m² are being found. Spenceley reports a spacing of about 6 cm outside 3 m from the trunk, corresponding with 250/m², while Bird shows values of less than 100/m². Pneumatophore diameters are estimated about 0.5 cm, while the height can reach values between 0.15 and 0.25 m. The C_D-value for these small rods in real waves can be assumed 1. With an assumed height of 0.2 m and a density varying between 50/m² and 400/m², this leads to a range of C_r-values of 0.025 to 0.2 (using equation (5)).

There is hardly any quantitative information on Rhizophora roots. Sato, 1989 has done some measurements on the dimensions of Rhizophora stilt roots. These, parabolically shaped roots, see Figure 1, reach up till 0.5 - 1 m above the ground, giving an average length of about 0.5 - 1 m. The average diameter varied from 2 - 3 cm, while the average number of roots in the first 0.5 m above the ground varied from 10 - 200. This gives a total root area per tree between 0.1 and 6 m². Combining the lower limits with small trees of 0.05 m and the upper limits with large trees of 0.25 m, we find from equations (6) and (5) 0.03 - 0.15 as a range for C_r.

A parametric study was done with HISWA, varying waterdepth, wave period, bottom friction and pile resistance with the limit values derived above. To avoid an avalanche of data, some restraints were observed. Firstly, the bottom was assumed to be horizontal; variation of slope will be discussed later on in this paper. Secondly, the wave transmission through a forest of 100 m wide will be presented. This wave transmission is simply defined as:

$$K_T = \frac{H_{ST}}{H_{SI}} \tag{7}$$

where H_{SI} is the incoming significant wave height (boundary condition in HISWA) and H_{ST} the calculated significant wave height after 100 m. For an arbitrary width of X m, K_T can be approximated with:

$$K_X = K_{100} \frac{X}{100} \tag{8}$$

Finally, the incoming wave height, H_{SI}, is coupled to the waterdepth. It has been said already that mangrove forests exist along coasts with moderate to low wave energy. They are either sheltered by foreshores, spits or mudflats where wave energy is dissipated. In order to avoid additional dissipation due to breaking in the computations, H_{SI} = 0.4*d was chosen.

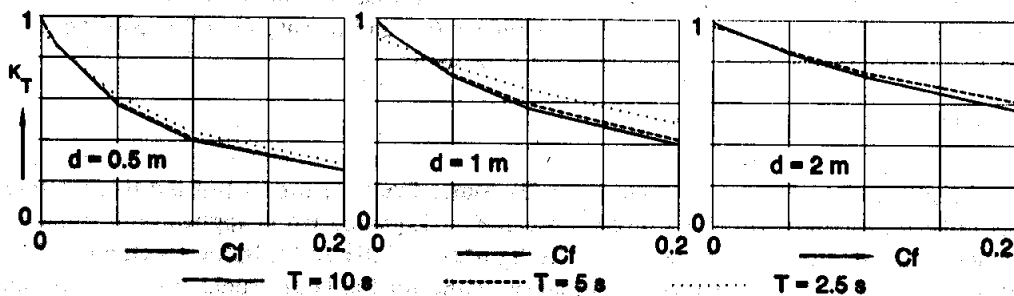


Figure 4 Wave transmission as a function of friction

The results of the computations for variation in friction are presented in Figure 4. The following can be seen in this figure:

1. Transmission increases with increasing waterdepth, due to a decreasing orbital motion at the bottom.
2. Transmission increases somewhat with decreasing wave period, again due to a decreasing orbital motion at the bottom, except with very low C_r -values when breaking of the steeper waves dominates. (Note: $T = 2.5$ s is not used in 2 m waterdepth since a wave of $H_s = 0.4 \cdot 2 = 0.8$ m would be too steep for that period).

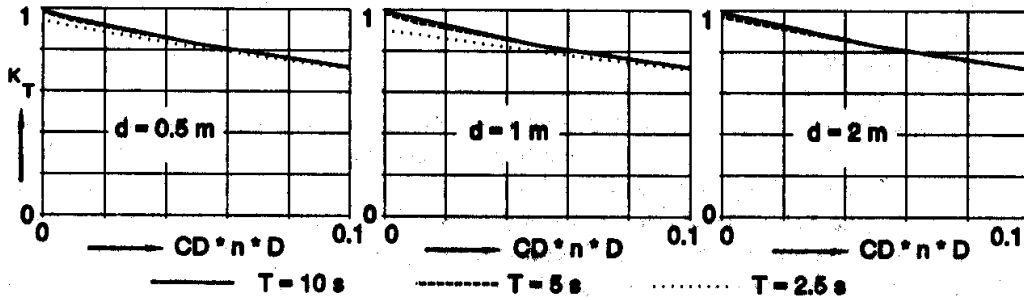


Figure 5 Wave transmission as a function of pile resistance

Figure 5 gives the results of the computations for pile resistance:

1. Transmission does not vary with waterdepth, the piles act over the full depth.
2. Transmission decreases somewhat with decreasing wave period, see equation (3).

From both figures the following conclusions can be drawn:

1. In the possible range for friction and drag in mangrove forests, as derived before, the effect of the roots dominates clearly over the effect of the trunks.
2. The influence of the wave period in both cases is small.

In order to restrict the amount of computational work further, only one wave period, $T = 5$ s, will be applied in the following. Taking into account the small contribution of the trunks, only one value for pile resistance will be used: $C_D \cdot n \cdot D = 0.03$, being an average of the values derived from equation (6). For the roots, three "archetypes" will be used: "sparse" $C_r = 0.025$, "average" $C_r = 0.05$ and "dense" $C_r = 0.1$. The available data make it unwarranted to make any distinction between *Avicennia* and *Rhizophora* forests, although there probably will be. This range has no other pretention than to obtain an idea of possible wave transmission.

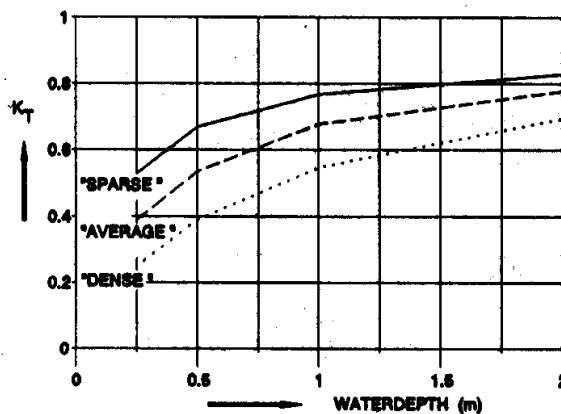


Figure 6 Wave transmission through 3 possible mangrove forests (100 m wide)

Figure 6 gives the result for the transmission (again for 100 m of mangroves and $H_s = 0.4d$).

Wave damping is quite effective at small waterdepths, but with high waterlevels, most wave energy is transmitted (the possible influence of branches and leaves has not been taken into account). This would mean that mangroves can have a significant influence on sedimentation during a large part of the tidal cycle, but are not very effective as breakwater. The latter seems in line with the findings of e.g. Sauer, 1962 and Jennings and Coventry, 1973 who report severe damage of vegetation behind mangroves, while the mangroves themselves were not or hardly damaged.

5. SHORE SLOPES

Among biologists and ecologists there has been much discussion whether mangroves are able to act as "land-builders". E.g. Davis, 1940 states that the seedlings can settle on the mud flats in front of the mangroves, giving a raise of the bottom level by sedimentation and organic waste material. Others, like Scholl, 1968, say that mangroves simply follow the changes in coastal morphology. Once the bottom level is high enough, mangroves will settle. Bird, 1972 says that mangroves need a certain bottom level to settle, but after that they are able to raise the bottom level. This could be caused by the wave damping, creating an environment in which sediment can more easily settle.

An assumption often made with sandy beaches is the idea of equal energy dissipation per unit area as proposed by Bruun, 1954. The idea is that, regardless of the process of sand movement perpendicular to the coast line, the breaking waves will "allow" a certain depth such that the energy dissipation is equal at every location. This leads to a parabolic curve for the beach profile. Outside the breakerzone things are more complicated, since there the process is no longer dominated by the violence of the breaking, but by a more subtle combination of velocity, boundary layer and fall velocity of the sand. On a mud coast, however, the sediment is so fine that it is not impossible that the assumption of equal energy dissipation is also valid outside the breaker zone. The sediment is getting into suspension quite easily and the wave energy dissipation again determines the waterdepth. (On unconsolidated mud coasts a completely different mechanism can be present. The waves can attenuate into the muddy bottom and wave energy is dissipated by internal work in the mud layer. This has not been taken into account here.)

Although these processes are outside the scope of this paper, some observations on wave energy dissipation from the HISWA program will be presented here.

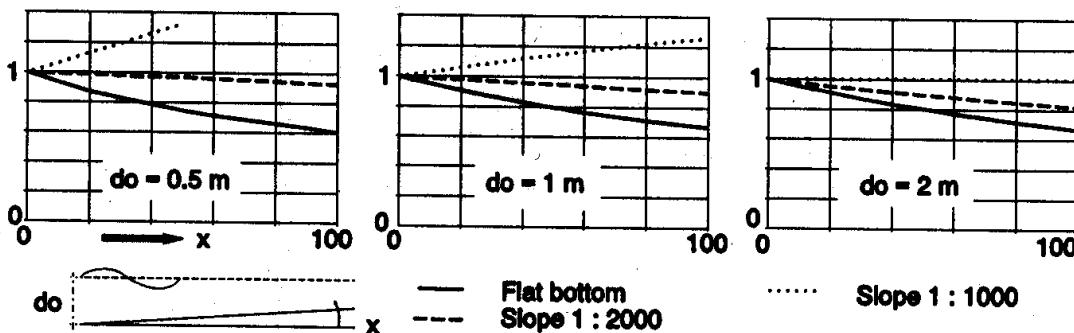


Figure 7 Energy dissipation divided by dissipation at boundary on bare slope ($C_r = 0.005$)

At first, the energy dissipation on a bare coast will be studied. Mud flats are usually rather smooth. Jonsson, 1966 gives for a hydraulically smooth bottom a friction factor C_f :

$$C_f = 0.09 + Re^{-0.2} \quad (Re = \frac{U_{max} \cdot a_b}{\nu}) \quad (9)$$

With waterdepths and the accompanying wave conditions as encountered here, a typical value of $C_f = 0.01$ (equivalent with a HISWA $C_f = 0.005$) is found. With this value and again $H_s = 0.4d$, computations were made with a flat bottom and varying slope, starting with the same waterdepth, d_0 , see Figure 7. In this figure a slope of 1:2000 to 1:1000 gives an equal energy dissipation per m^2 along the slope.

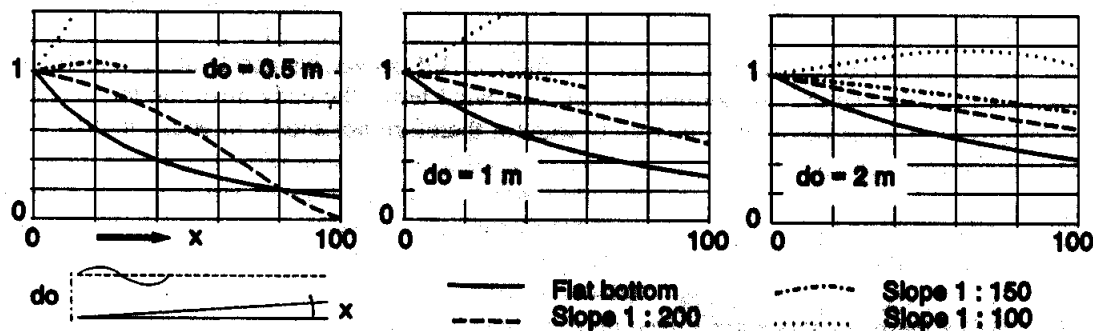


Figure 8 Energy dissipation per m^2 along slope divided by energy dissipation at boundary with "average" mangrove vegetation ($C_f = 0.05$)

The same was done for the three "archetypes" of mangrove forests. The results for the case "average" vegetation, see Figure 6, are presented in Figure 8. Now a slope of around 1:150 gives an equal wave energy dissipation per m^2 . For "sparse", the slope for equal dissipation was found to be 1:300 to 1:200 and for "dense" 1:100 to 1:75. Of course, the real situation is much more complex with changing waterlevels and wave conditions, so these numbers can be no more than an indication.

Bird, 1972 reports on slopes in Australia. He found for the mud flats in front of mangroves slopes of "1:1000 or less". In zones with *Avicennia* he reports slopes between 1:150 and 1:300 and for *Rhizophora* 1:500. In another area he reports a slope of 1:50 in an *Avicennia* zone (Bird, 1980). As said before, the available data on trees and roots are not detailed enough to discriminate between *Avicennia* and *Rhizophora*. The same is true for the reported slopes, so only a rough impression of the relation between slope and vegetation can be presented here.

In this paper it suffices to say that the relations, as found from the HISWA computations, are in line qualitatively with what is found in nature and are interesting enough to take into account in future considerations on coasts with mangroves. The statement that mangroves can raise the bottom level, once they are settled, seems reasonable.

6. LONG WAVE TRANSMISSION AND THE DUCHESS/DUFLOW PROGRAMS

For long waves, DUT has available two mathematical models: DUCHESS (Delft University Computer program for 2-dimensional Horizontal Estuary and Sea Surges), see Booij, 1990 and DUFLOW (DUtch FLOW) for 1-dimensional computations, see Spaans and Booij, 1989.

Both models are based on the equation of motion for gradually varying horizontal flow and the continuity equation. In DUCHESS, the equation of motion for the X-direction reads (in the Y-direction a similar equation is applied):

$$\frac{\partial q_x}{\partial t} + \frac{\partial(q_x^2/d)}{\partial x} + \frac{\partial(q_x q_y/d)}{\partial y} + g d \frac{\partial h}{\partial x} + g \frac{q_x \sqrt{q_x^2 + q_y^2}}{Ch^2 d^2} = 0 \quad (10)$$

where the 1st term represents local inertia, the 2nd and 3rd convective acceleration, the 4th waterlevel gradient and the 5th bottom friction. The wind term, the eddy diffusion terms and the Coriolis term were not used in this study and are therefore not shown in equation (10). The continuity equation reads:

$$\frac{\partial h}{\partial t} + \frac{\partial q_x}{\partial x} + \frac{\partial q_y}{\partial y} = 0 \quad (11)$$

In DUCHESS these equations are solved on a rectangular grid.

In DUFLOW the same basic equations are applied in a network of branches and nodes, but restricted to the x-direction, integrated over the width perpendicular to the flow direction. The equations of motion and continuity read:

$$\begin{aligned} \frac{\partial Q}{\partial t} + \frac{\partial(Qu)}{\partial x} + gA \frac{\partial h}{\partial x} + g \frac{|Q|Q}{Ch^2 Ad} &= 0 \\ B \frac{\partial h}{\partial t} + \frac{\partial Q}{\partial x} &= 0 \end{aligned} \quad (12)$$

The flow in these branches is parameterized by making a distinction between the stream width and the storage width in a branch. B is the total width of the wetted cross-section; it is used in the continuity equation. The stream width, A/d, is the part of the branch where the water really flows and is used in the equation of motion.

The resistance of trees can be incorporated in the equation of motion by applying the same expression for the drag force as used in equation (2). This extra term is implemented in DUCHESS but not yet in DUFLOW. In DUFLOW, the effect of trees has to be included in the bottom friction term. This can be done in the same way as in equation (5). This leads to an expression for the Chezy coefficient:

$$Ch = \sqrt{\frac{2g}{nC_D Dd}} \quad (13)$$

DUCHESS is superior to DUFLOW because of the extra dimension in the equations. This extra dimension is probably important in estuaries with large areas being flooded during tides or storm surges. On the other hand, the use of 2-dimensional models like DUCHESS for a vast

area with a "real world" schematization is expensive and time-consuming, both in schematizing and computing. For preliminary studies it can therefore be attractive to use a 1-dimensional model. This paper will focus on the question how to schematize a river with vegetated flood plains, which also take part in the flow, for a 1-dimensional model. To answer this question, a comparison is made between DUCHESS and DUFLOW. The results of DUCHESS will be used as standard to judge the outcomes of the DUFLOW computations.

For the comparison it is sufficient to use a fictitious and/or simplified case. The choice for the case was inspired by the situation as found in the Sunderbans in Bangladesh, where rivers flow through thousands of km² of vegetated islands that can be flooded. The Sunderbans could even serve as a protection for the mainland North of it by damping the surges induced by cyclones in the Bay of Bengal.

As standard case, a river of 60 km long, 6 m deep (below MSL) and 1700 m wide was taken (more or less based on rivers in the Sunderbans). The width of the flood plains is taken 15000 m. To investigate the differences between DUCHESS and DUFLOW, two different geometries of the river were taken, one with a sloping and one with a flat flood plain, see Figure 10.

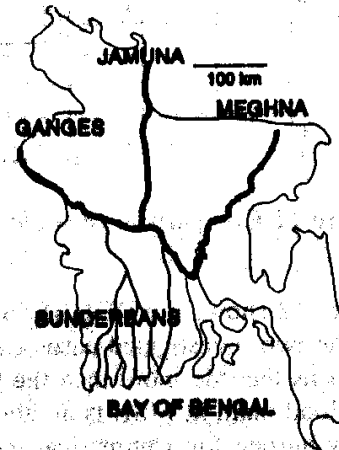


Figure 9 Bangladesh

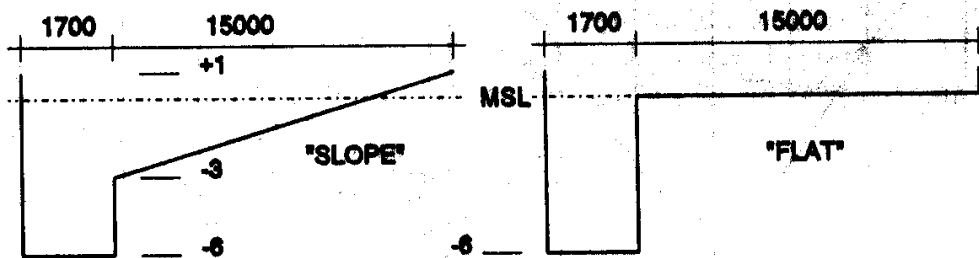


Figure 10 Investigated river cross-sections

As boundary condition for the tidal computation, a simple sine function with an amplitude of 0.75 m and a period of 12 hours at the sea-side of the estuary was taken. At the other side, the estuary was assumed to be closed with no river discharge. This seems unrealistic, but it should be kept in mind that the purpose is to compare the behaviour of a tidal wave in a schematized case between a 2-dimensional and a 1-dimensional model.

As said before the resistance of trees can not yet be included separately from the bottom friction effect in DUFLOW. From equation (13) we can see that the resistance increases with increasing waterdepth (lower Chezy-value). When the extra resistance due to trees is incorporated in the bottom friction, this effect gets lost. Therefore, before comparing DUFLOW and DUCHESS, we compare the results with separate tree resistance, schematized as pile drag, and a fixed Chezy-value in DUCHESS. Figure 11 shows the computational results for a point inside the area, 10 km from the boundary for trees with $D = 0.15$ m, $n = 0.057/m^2$ and a fixed Ch-value $= 20 \sqrt{m/s}$. The differences are small, but, in order to make a pure comparison between

DUCHESS and **DUFLOW**, a fixed Ch -value = 20 will be used in both models.

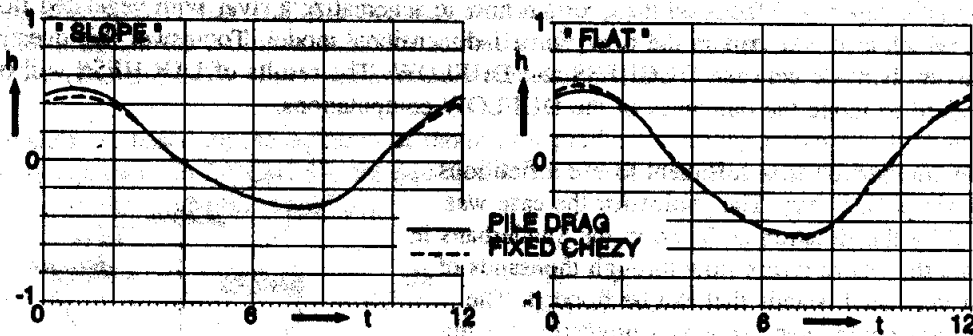


Figure 11 Comparison separate vegetation resistance with fixed Chezy-value in **DUCHESS**

Figure 12 shows the **DUCHESS**-results for the waterlevel at various locations along the river for the two investigated cases from Figure 10. It can be seen that the sloping flood plain dampens the tide more than the flat plain, the latter being "active" only part of the time. The flat flood plain at MSL is an abrupt change in the geometry of the river branch and forms a heavy burden for a numerical model, resulting in a less smooth waterlevel curve at the rear end of the estuary.

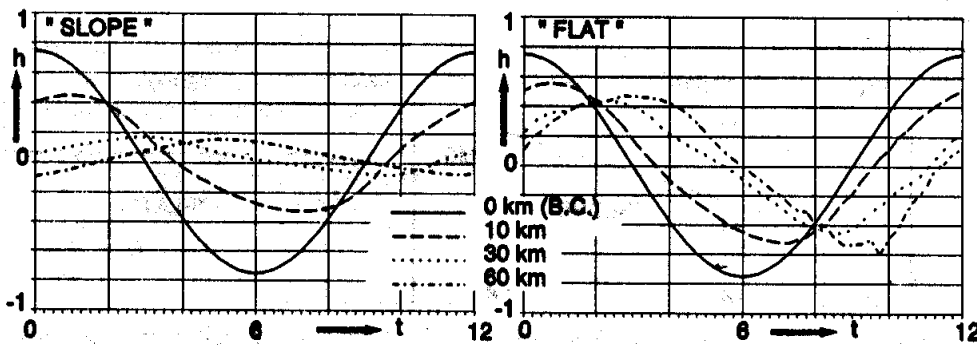


Figure 12 Transmission of tidal wave as computed with **DUCHESS**

As a first check, both models were run with only the main branch of the river (60 km long, 6 m deep, 1700 m wide, $Ch = 50$, without flood plains). The results were identical as could be expected. For the comparison of the two situations of Figure 10, three types of 1-dimensional schematizations were applied, see Figure 13.

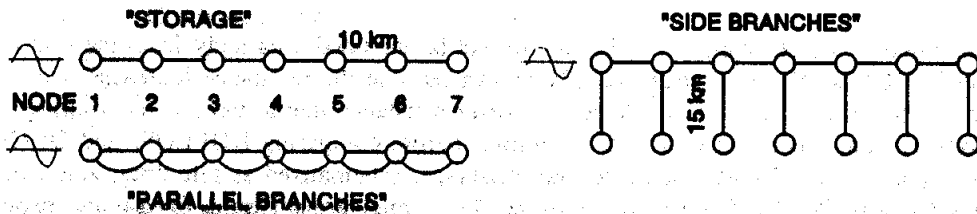


Figure 13 1-dimensional schematizations

In the first case the river is schematized with single branches with a Chezy-value of $50\sqrt{m/s}$. The vegetated flood plains were schematized as storage width of the river.

In the second case, the main branch of the river is schematized with the same Chezy-value, but without storage area. The vegetated flood plains were schematized as parallel branches with the same length as the main branches, a Chezy-value of 20 and a width equal to the storage width of the first case.

In the third case, the river was taken equal to the second case, while the flood plains were schematized as side branches with a length equal to the storage width of the first case, a Chezy-value of 20 and a width equal to the length of the main branches.

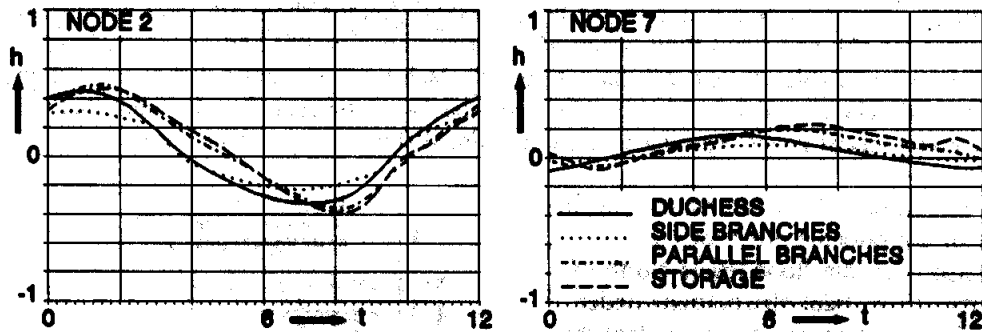


Figure 14 Comparison DUFLOW-DUCHESS for vegetated flood plain "SLOPE"

The results for the case with a sloping flood plain are presented in Figure 14.

None of the 1-dimensional schematizations gives an accurate description of the 2-dimensional results, but for a preliminary idea none of them is unacceptable either. In practice, a 1-dimensional model is always tuned to measurements by adjusting the Ch-value, giving often reasonable results.

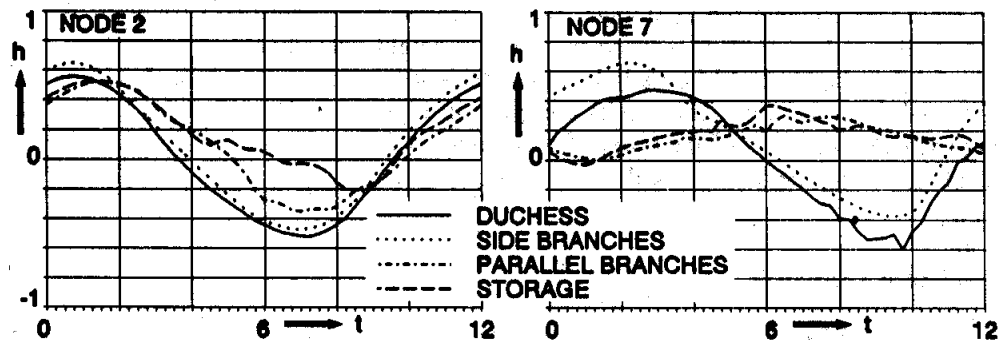


Figure 15 Comparison DUFLOW-DUCHESS for vegetated flood plain "FLAT"

The results for the case with a flat flood plain are given in Figure 15. Numerical problems in DUFLOW, analogous to those in DUCHESS, made it necessary to use some extra tricks. The case with storage could not be performed with the abrupt change as in DUCHESS, but the increase in extra storage width from 0 to 15000 m had to be done in 1 m height. Drying nodes and branches are not possible in DUFLOW, so the parallel branches needed a very small channel below LW, while the side branches were equipped with a weir between them and the main branches with a crest at MSL. The similarity for the cases with storage and parallel

branches is now far from good, but is quite reasonable for the case with side branches. Apparently, the flow is dominated by critical flow from the flood plain into the main branch during LW, which is described accurately enough by the flow over the weir in the 1-dimensional model. The similarity with side branches in the case of the sloping flood plain, see Figure 14, was much less, so, in that case the flow is of a true 2-dimensional nature.

From these results it becomes obvious that for a good schematization of the flow in an estuary with large vegetated flood plains, a 2-dimensional model is needed. Since, however, the situation with the flat flood plain is very extreme and since adjustments are possible a 1-dimensional model can give satisfactory results for a preliminary study. Experience learns that sometimes various "tuning gadgets" can be necessary. Among those are the Ch-value, different Ch-values for ebb and flood flow, weirs with various crest widths and/or levels. A universal recipe is not available, so one will have to decide each time whether a 1-dimensional approach is still valid. The comparison between the two models can be seen as a warning that a 1-dimensional model never reproduces a 2-dimensional flow situation completely.

With this in mind, a rough estimation was made of the possible effect of the Sunderbans on the flood levels North of the area. From tidal observations under normal circumstances, it appears that the amplitude 60 km inland is practically the same as at the sea boundary. This indicates that the bottom levels of the majority of the area is higher than HW, see also Figure 12 (indicating also that the trees growing there will probably other than mangroves, see section 2). The area was schematized simply with the main branch as in the other examples, while the flood plain was schematized as storage, starting around HW, with two variations: the full storage width of Figure 10 is reached in 1 or 2 m height respectively. As boundary condition a surge of 1.5 m high and 12 hours long was superposed on the normal tide, based on rough information from the area. The results are given in Figure 16. The effect for both cases of storage schematization is of the order of magnitude of 0.5 m. To the authors, no data are available at the moment to check this outcome.

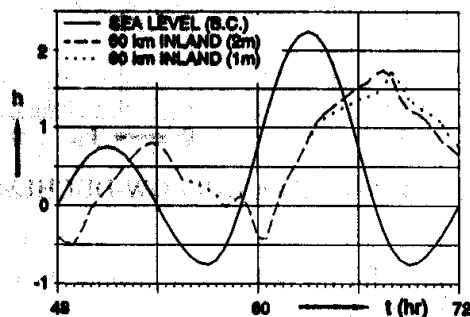


Figure 16 Waterlevel during possible cyclone in the Sunderbans

7. CONCLUSIONS

- 1 The HISWA model reproduces satisfactorily measurements of wave transmission through pile arrays in a laboratory flume.
- 2 The root systems of *Rhizophora* and *Avicennia* mangroves seem to have a greater effect on wave damping than the trunks. This also means that the wave damping decreases with increasing waterdepth.
- 3 The wave period has little influence on the wave transmission.
- 4 For waterdepths less than 1 m, wave damping in a mangrove forest of 100 m wide lies possibly around 50 %. The orbital velocities will be lowered with the same percentage,

indicating that the conditions for sedimentation will be more favourable.

- 5 For larger waterdepths, the wave damping lies around 20 - 30 %. The effect of mangroves as natural breakwaters during surges is therefore limited.
- 6 Starting from a hypothesis of equal energy dissipation per m^2 , the bottom slope in a mangrove forest can be steeper than without mangroves. This is in line with what is found in nature.
- 7 For accurate tidal computations in estuaries where inundation of and flow through large areas of vegetated flood plains play an important role, a 2-dimensional model is needed. For preliminary studies, 1-dimensional computations can be sufficient.
- 8 The influence of the Sunderbans on cyclone surge levels seems limited.

NOTATION

a	wave amplitude	m
a_b	wave amplitude at bottom	m
$c_{x,y}$	propagation speed in x,y-domain	m/s
c_θ	propagation speed in θ -domain	1/s
d	waterdepth	m
g	acceleration of gravity	m/s^2
h	waterlevel (with regard to reference level)	m
k	wave number (= $2\pi/\lambda$, λ = wavelength)	1/m
n	number of piles per unit area	$1/m^2$
q	depth integrated velocity	m^2/s
t	time	s
u	velocity	m/s
x	horizontal coordinate	m
y	horizontal coordinate	m
z	vertical coordinate	m
A	area of cross section	m^2
B	storage width	m
C_D	drag coefficient	-
C_F	friction coefficient	-
C_r	friction coefficient (in HISWA (= $1/2 C_F$))	-
Ch	Chezy coefficient	$\sqrt{m/s}$
D	diameter of pile	m
E	wave energy (variance) density	m^2/s
H	wave height	m
K	wave transmission coefficient	-
L	length of pile	m
Q	area integrated velocity, discharge	m^3/s
S	sink term of wave energy (variance)	m^2/s
T	wave period	s
W	work	kgm^2/s^2
ν	viscosity	m^2/s
θ	wave direction	-
τ	shear stress	$kg/m.s^2$
ω	circular frequency (= $2\pi/T$)	1/s

REFERENCES

- Battjes, J.A. and Janssen, J.P.F.M., 1979 Energy loss and set-up due to breaking of random waves, Proc. 16th Int. Coastal Eng. Conference, 1978, Hamburg. ASCE, N.Y., pp 569-587
- Bird, E.C.F., 1972 Mangroves and Coastal Morphology in Cairns Bay, North Queensland, Journal of Tropical Geography 35, pp. 11-16
- Bird, E.C.F., 1980 Mangroves and Coastal Morphology, Victoria Naturalist, Vol.97
- Booij, N., 1990 DUCHESS User manual
- Bruun, P., 1954 Coast erosion and the development of beach profiles, Memorandum no 44, US Army Corps of Engineers, Beach Erosion Board, Washington D.C.
- Davis, J.H., 1940 The ecology and geologic role of mangroves in Florida, Pap. Tortugas lab., Vol. 32, no 16, pp. 307-409
- Groen, R.A., 1993 Mangroves as coastal defence (in Dutch), MSc-thesis Delft University of Technology
- Heidemann, J.C. and Sarpkaya, T., 1985 Hydrodynamic forces on dense arrays of cylinders, 17th Annual Offshore Technology Conference, Houston, pp 421-428
- Holthuijsen, L.H., Booij, N. and Herbers, T.H.C., 1989 A prediction model for stationary, short crested waves in shallow water with ambient currents, Coastal Engineering, 13, pp 23-54
- Hopley, 1974 Coastal changes produced by tropical cyclone Althea in Queensland, The Australian Geographer, 1974
- Ippen et al. 1962 Some characteristics of wave filters composed of circular cylinders, Appendix to: Wave induced oscillations in harbors, Effects of energy dissipators in coupled basin systems, Report nr 52, Massachusetts Institute of Technology
- Jennings, J.N. and Coventry, R.J., 1973 Structure and texture of a gravelly barrier island in the Fitzroy Estuary, Western Australia and the role of mangroves in the shore dynamics, marine Geology, 15, pp 145-167
- Jonsson, I., 1966 Wave boundary layers and friction factors, Proc. Int. Coastal Eng. Conference, pp 127-148
- Noakes, D.S.P., 1955 Methods of increasing growth and obtaining natural regeneration of the mangrove type in Malaya, Malaysian Forester, no 18, pp. 23-30
- Putnam, J.A. and Johnson, J.W., 1949 The dissipation of wave energy by bottom friction, Transactions American Geophysical Union, 30: 67-74
- Sato, 1985 Studies on the protective functions of the mangrove forests against erosion and destruction V, Preliminary trials of the mangrove forests as a coastal prevention forest, Science Bulletin Agricultural University of the Ryukyus, no 32 pp 161-172
- Sato, 1989 Studies on stilt root of Rhizophora Stylosa and properties of sedimentation in mangrove forest, Galaxea, 8:43-48
- Sauer, 1962 Effects of recent tropical cyclones on the coastal vegetation of Mauritius, Journal of Ecology
- Scholl, D.W., 1968 Mangrove swamps: geology and sedimentology, The encyclopedia of geomorphology, R.W.Fairbridge (ed.), Reinhold Book Corporation, New York, pp 683-688
- Snedaker, S.C. and Snedaker, J.G., 1984 The Unesco/SCOR Working Group 60 on Mangrove Ecology, "The Mangrove Ecosystem Research Method"
- Spaans, W. and Booij, N., editors, 1989 DUFLOW User manual
- Spenceley, A.P., 1977 The role of pneumatophores in sedimentary processes, marine Geology, 24 M31-M37
- Steinke, T.D. and Ward, C.J., 1989 Some effects of the cyclones Domoina and Imboa on mangrove communities in the St. Lucia Estuary, S.-Afr. Tydskr. Plantk., 55(3), pp 340-348
- Stoddart, 1965 Re-survey of hurricane effects on the British Honduras reefs and cays, Nature, 207, pp. 589-592